



**Toxicity of Layered Semiconductor Chalcogenides:  
Beware of Interferences**

Journal:	<i>RSC Advances</i>
Manuscript ID:	RA-ART-05-2015-009404.R2
Article Type:	Paper
Date Submitted by the Author:	29-Jul-2015
Complete List of Authors:	Latiff, Naziah Binte Mohamad; Nanyang Technological University, Teo, Wei Zhe; Nanyang Technological University, Chemistry and Biological Chemistry Sofer, Zdenek; Institute of Chemical Technology, Prague, Department of Inorganic Chemistry Huber, Štěpán; Institute of Chemical Technology Prague, Department of Inorganic Chemistry Fisher, Adrian; University of Cambridge, Chemical Engineering and Biotechnology Pumera, Martin; Nanyang Technological University, Chemistry and Biological Chemistry

# Toxicity of Layered Semiconductor Chalcogenides: Beware of Interferences

**Naziah Latiff<sup>a</sup>, Wei Zhe Teo<sup>a</sup>, Zdenek Sofer<sup>b</sup>, Štěpán Huber<sup>b</sup>, Adrian C. Fisher<sup>c</sup>, Martin Pumera<sup>a\*</sup>**

<sup>a</sup>Division of Chemistry & Biological Chemistry, School of Physical and Mathematical Sciences, Nanyang Technological University, Singapore 637371, Singapore.

<sup>b</sup>Institute of Chemical Technology, Department of Inorganic Chemistry, Technická 5, 166 28 Prague 6, Czech Republic.

<sup>c</sup>Department of Chemical Engineering and Biotechnology, University of Cambridge, New Museums Site, Pembroke Street, Cambridge CB2 3RA, United Kingdom.

\* E-mail: [pumera@ntu.edu.sg](mailto:pumera@ntu.edu.sg); Fax: (+65)6791-1961

**Abstract**

The absence of bandgap in graphene has opened exploration in a new class of 2D nanomaterials: layered semiconductor chalcogenides. Research has found that they have promising properties which are advantageous for applications in a wide range of fields such as solar energy conversion, field effect transistors, optoelectronic devices, energy storage, and is expanding into biomedical applications. However, little is known about their toxicity effects. In view of the possibility of employing these materials into consumer products, we investigated the cytotoxicity of two common layered semiconductor chalcogenides, namely GaSe and GeS, based on cell viability assessments using water-soluble tetrazolium salt (WST-8) and methyl-thiazolyldiphenyl-tetrazolium bromide (MTT) assays after a 24 h exposure to varying concentrations of the nanomaterials on human lung carcinoma epithelial cells (A549). The cytotoxicity results indicated that GaSe is relatively more toxic than another group of 2D layered chalcogenide: transition metal dichalcogenides ( $\text{MoS}_2$ ,  $\text{WS}_2$ ,  $\text{WSe}_2$ ). On the other hand, GeS appeared to be non-toxic, with concentration of GeS introduced having a positive correlation with the cell viability. Control experiments in cell-free conditions revealed that both GaSe and GeS interfered with the absorbance data gathered in the two assays, but the interference effect induced by GaSe could be minimized by additional washing steps to remove the nanomaterials prior to the cell viability assessments. In the case of GeS, however, the interference effect between GeS and both assay dyes were still significant despite the washing steps adopted, thereby giving rise to the false cytotoxicity results observed for GeS. Therein, we wish to highlight that control experiments should always be carried out to check for any possible interferences between test specimen and cell viability markers when conducting cell viability assessments for cytotoxicity studies.

## 1. Introduction

Two-dimensional (2D) layered nanomaterials have received much attention since the successful isolation of graphene from graphite.<sup>1,2</sup> They typically possess unique and distinct properties from their three-dimensional (3D) forms. As one of the first prototypes of layered structures, research on 2D materials has been predominated by graphene. Graphene is a single layer of  $sp^2$  carbon atoms bonded hexagonally together, with high surface area, high mechanical strength, high elasticity, and fast heterogeneous electron transfer.<sup>Error! Bookmark not defined.</sup> However, the absence of an intrinsic bandgap has limited its application in nanoelectronic and optoelectronic devices. To overcome this, alternative 2D materials have been explored to find new possible opportunities for specific applications.

Recently, a new stable class of 2D materials; semiconductor Group III and Group IV chalcogenides has been studied. They contain an element from either Group III or Group IV element (e.g. Ga, Ge, In, Sn, Tl) and a chalcogen (eg. S, Se or Te). These materials have opened a new fascinating chapter in nanoelectronic applications. For example, gallium selenide (GaSe) and germanium sulfide (GeS) have been reported to have suitable properties, such as thermal, mechanical and photostability, for a wide range of potential applications ranging from solar cells, field effect transistors, photodetectors, infrared light-emitting diodes, cutoff devices, enhanced lithium ion batteries, fiber optics, sensors and optical lenses for infrared transmission.<sup>1,2,3-14</sup> Furthermore, their suitability as optical fibres as well as photodetectors, have triggered efforts to extend these applications towards the biomedical field such as medical diagnosis.<sup>15,16</sup> With the rise in research and possible commercialization of this group of materials in the future, it is therefore necessary to investigate their toxicological effects in order to be informed of any potential health hazards that they may pose.<sup>17</sup>

Currently, to the best of our knowledge, even though there have been toxicity reports found for Ga- and Ge- containing compounds<sup>18-21</sup>, no toxicity assessments were performed on GaSe and GeS specifically. For instance, copper gallium diselenide (CGS), used in photovoltaic and semiconductor industries, was reported to leach gallium and selenide ions in the lung tissues of rats after 24 h intratracheal instillation of the material, causing mild transient inflammatory response in the lung.<sup>19</sup> For Ge, some reactive germanium intermediate compounds have been reported to be poisonous, while some germanium compounds showed low toxicity.<sup>20,21</sup> Since toxicity data on GaSe and GeS is unexplored, we aim to investigate the toxicological effects of GaSe and GeS, for the first time, on the human lung carcinoma epithelial cell line (A549) through *in vitro* studies of cell viability after 24 h exposure to these semiconductor chalcogenides. A549 cells were chosen for the cytotoxicity assessment as the lungs are likely to be the first point of contact with the body when these nanomaterials enter through inhalation.

Various concentrations of the nanomaterials were tested to study the effect of concentration on their cytotoxicity. After a 24 h incubation with GaSe and GeS, the viability of cells was analyzed using two assays: water-soluble tetrazolium salt (WST-8) and methyl-thiazolyldiphenyl-tetrazolium bromide (MTT). These two well-established cell viability assays produce coloured formazan dyes in the presence of metabolically active cells.<sup>22</sup> The amount of cells that remained viable after exposure to the nanomaterials can then be determined using absorbance spectroscopy. With the utilization of two cell viability assays that work on similar principles, misinterpretation of the absorbance data could be avoided.<sup>23</sup>

## Experimental and methods

### Apparatus

The SEM images were obtained from a JEOL 7600F field-emission scanning electron microscopy (JEOL, Japan) with an accelerating voltage of 2.00 kV, and a working distance of 5.9 mm under Gentle Beam mode, while the STEM images were obtained from the same equipment using an accelerating voltage of 30.00 kV, and a working distance of 8.3 mm under SEM mode. 0.1 mg/mL samples in dimethylformamide (DMF) were prepared for the STEM imaging. EDS was obtained using Oxford instruments x-stream2 and micsf+ with an accelerating voltage of 30.00 kV. X-ray powder diffraction data were collected at room temperature with an X'Pert PRO  $\theta$ - $\theta$  powder diffractometer with parafocusing Bragg-Brentano geometry using Cu K $\alpha$  radiation ( $\lambda = 0.15418$  nm, U = 40 kV, I = 30 mA). Data were scanned with an ultrafast detector X'Celerator over the angular range 5 – 80  $^{\circ}2\theta$  with a step size of 0.0167  $^{\circ}2\theta$  and a counting time of 20.32 s step $^{-1}$ . Data evaluation was performed in the software package HighScore Plus.

### Chemicals

Germanium (99.999%), gallium (99.999%), selenium (99.999%) and sulfur (99.999%) were obtained from STREM, USA. Quartz glass ampoules were washed with hydrofluoric acid, deionized water and acetone before use. Subsequently, the ampoules were heated by hydrogen/oxygen torch under high vacuum (below  $5 \times 10^{-3}$  Pa) to remove any contamination. Methyl-thiazolyldiphenyl-tetrazolium bromide (MTT) was purchased from Sigma-Aldrich. Water-soluble tetrazolium salt (WST-8) was purchased from Dojindo. Dimethyl sulfoxide (DMSO) was purchased from Tedia. Dulbecco's Modified Eagle medium and phosphate buffer solution (PBS), pH 7.2 were purchased from Gibco. Fetal bovine serum and 1% penicillin-streptomycin liquid were purchased from PAA Laboratories.

### **Synthesis of GaSe and GeS**

For the GaSe synthesis, 15 g stoichiometric mixture of granulated Ga and Se was placed in quartz glass ampoules (25 mm x 150 mm) and evacuated below  $5 \times 10^{-3}$  Pa using diffusion pump. Evacuated ampoule was sealed using oxygen-hydrogen torch. Reaction mixture was heated at a rate of 1 °C/min. After 48 h at 850 °C, the reaction mixture was cooled and subsequently reheated to 970 °C at a rate of 1 °C/min. After 1 h at 970 °C, the reaction mixtures were cooled at a rate of 1 °C/min.

For GeS synthesis, 10 g stoichiometric mixture of granulated Ge and S was placed in quartz glass ampoules (25 mm x 150 mm) and evacuated below  $5 \times 10^{-3}$  Pa using diffusion pump. Evacuated ampoule was sealed using oxygen-hydrogen torch. Reaction mixture was heated at a rate of 1 °C/min. After 5 h at 700 °C, the reaction mixture was cooled at a rate of 1 °C/min.

### **Cell culture**

The human lung carcinoma epithelial cell line A549, a popular cell line in nanotoxicological studies, was used to determine the nanotoxicity of the GaSe and GeS. A459 cells have a typical cell cycle of 22 h and were purchased from Bio-REV Singapore. Cells were cultured with Dulbecco's Modified Eagle medium (DMEM) supplemented with 10% fetal bovine serum (FBS) and 1% penicillin-streptomycin liquid in an incubator maintained at 37°C under 5% CO<sub>2</sub>. The cells were seeded in 24-well plates (570 µL per well) with a cell density of  $8.8 \times 10^4$  cells per mL for 24 h before introducing the nanomaterials.

### **Cell exposure to GaSe and GeS**

After seeding, the culture medium was first removed and each well was rinsed with PBS (pH 7.2). The cells were then incubated with different concentrations (3.125, 6.25, 12.5, 25, 50,

100, 200, 400  $\mu\text{g/mL}$ ) of nanomaterial dispersions (570  $\mu\text{L}$  per well) for another 24 h. Cells incubated without nanomaterials were used as a negative control.

#### **WST-8 assay**

After 24 h incubation with the nanomaterials, the cells were washed twice with PBS (pH 7.2) and incubated with 10% diluted stock WST solution (300  $\mu\text{L}$  per well) at 37°C and 5%  $\text{CO}_2$  for 1 h. The solutions were subsequently centrifuged at 8000 rpm for 10 min to remove any traces of GaSe and GeS, before transferring 100  $\mu\text{L}$  of the supernatant to a 96-well plate to measure their absorbance at 450 nm and 800 nm (background absorbance).

#### **MTT assay**

After 24 h incubation with GaSe and GeS, the cells were washed twice with PBS (pH 7.2) and incubated with 1 mg/mL of MTT solution (300  $\mu\text{L}$  per well) at 37°C and 5%  $\text{CO}_2$  for 3 h. Thereafter, the MTT solution was removed and an equal volume of DMSO was added to dissolve the purple formazan crystals formed by the viable cells. The plates were gently agitated at 500 rpm for 5 min, and then the solutions were centrifuged at 8000 rpm for 10 min to remove any traces of the nanomaterials. Following centrifugation, 100  $\mu\text{L}$  of the supernatant were transferred to a 96-well plate and their absorbance were measured at 570 nm and 690 nm (background absorbance).

#### **WST-8 assay control experiment**

The different concentrations of GaSe and GeS in culture media were prepared and incubated with 10% diluted stock WST solution (300  $\mu\text{L}$  per well) in the absence of viable cells at 37°C and 5%  $\text{CO}_2$  for 1 h. Subsequently, the solutions were centrifuged at 8000 rpm for 10 min to remove any traces of nanomaterials, before transferring 100  $\mu\text{L}$  of the supernatant to a 96-well plate to measure their absorbance at 450 nm and 800 nm (background absorbance).



### MTT assay control experiments

Two control experiments were conducted. For the first control experiment, different concentrations of GaSe and GeS in culture media were prepared and incubated with 1 mg/mL MTT solution (500  $\mu$ L per well) in the absence of viable cells at 37°C and 5% CO<sub>2</sub> for 3 h. Thereafter, the MTT solutions were removed and an equal volume of DMSO were added to dissolve the purple formazan crystals formed by living cells. The plates were gently agitated at 500 rpm for 5 min, and then the solutions were centrifuged at 8000 rpm for 10 min to remove any traces of the nanomaterials. Following centrifugation, 100  $\mu$ L of the supernatant were transferred to a 96-well plate and their absorbance were measured at 570 nm and 690 nm (background absorbance).

For the second MTT control experiment, a set of 24-well plates containing 200  $\mu$ L of the above-mentioned cell-free MTT-nanomaterial solution (subjected to 3 h incubation at 37°C and 5% CO<sub>2</sub>) was prepared. 120  $\mu$ L of 4 mM of ascorbic acid was added to each well, and the solutions were mixed gently by agitation at 500 rpm for 5 min. Subsequently, the MTT-nanomaterial-ascorbic acid mixtures were incubated at 37°C and 5% CO<sub>2</sub> for 1 h. DMSO was then added to the mixtures at a ratio of 2 : 1 before incubating them for another 10 min. Finally, the solutions were centrifuged at 8000 rpm for 10 min, and their absorbance were measured at 570 nm and 690 nm (background absorbance).

## Results and discussion

### Material characterization

Characterization of GaSe and GeS nanomaterials were carried out by scanning electron microscopy (SEM), Energy-Dispersive X-ray spectroscopy (EDS), X-ray diffraction (XRD) and Scanning Transmission Electron Microscopy (STEM) to determine the morphology and elemental composition of the nanomaterials. This is necessary as toxicity of a nanomaterial have been reported to be associated to its physicochemical properties.<sup>24</sup>

SEM images in Figure 1 show that both GaSe and GeS nanomaterials are platelets of various dimensions, but are fairly similar in morphologies. In addition, STEM confirms that the platelets are few- to multi-layered. Both nanomaterials also exhibit similar diversity in their particle size distributions, with a large spectrum of platelet sizes ranging from approximately 20  $\mu\text{m}$  and 1  $\mu\text{m}$ . Since the particle size distributions of GaSe and GeS in this study are relatively comparable from the SEM and STEM images, we did not study the influence of particle sizes on the cytotoxicity of the materials.

Elemental composition analysis revealed that the ratio of M:X in GaSe and GeS was 1:1.0 and 1:1.2 respectively. In addition, trace amounts of magnesium (4.8 at.%) was found in GeS nanosheets, whereas GaSe was free from metal impurities. Figure 2 show the results of X-ray diffraction measurement. The samples were prepared for the measurement by mechanical grinding in agate mortar from bulk material. On both diffractograms, it is clearly visible that there is preferential orientation along (001) direction originating from highly anisotropic mechanical properties of layered materials.

Both materials are single phase with GaSe having hexagonal structure (space group  $P6_3/mmc$ ) and GeS exhibiting orthorhombic structure (space group  $Pbnm$ ). The corresponding structures are shown on Figure 2.

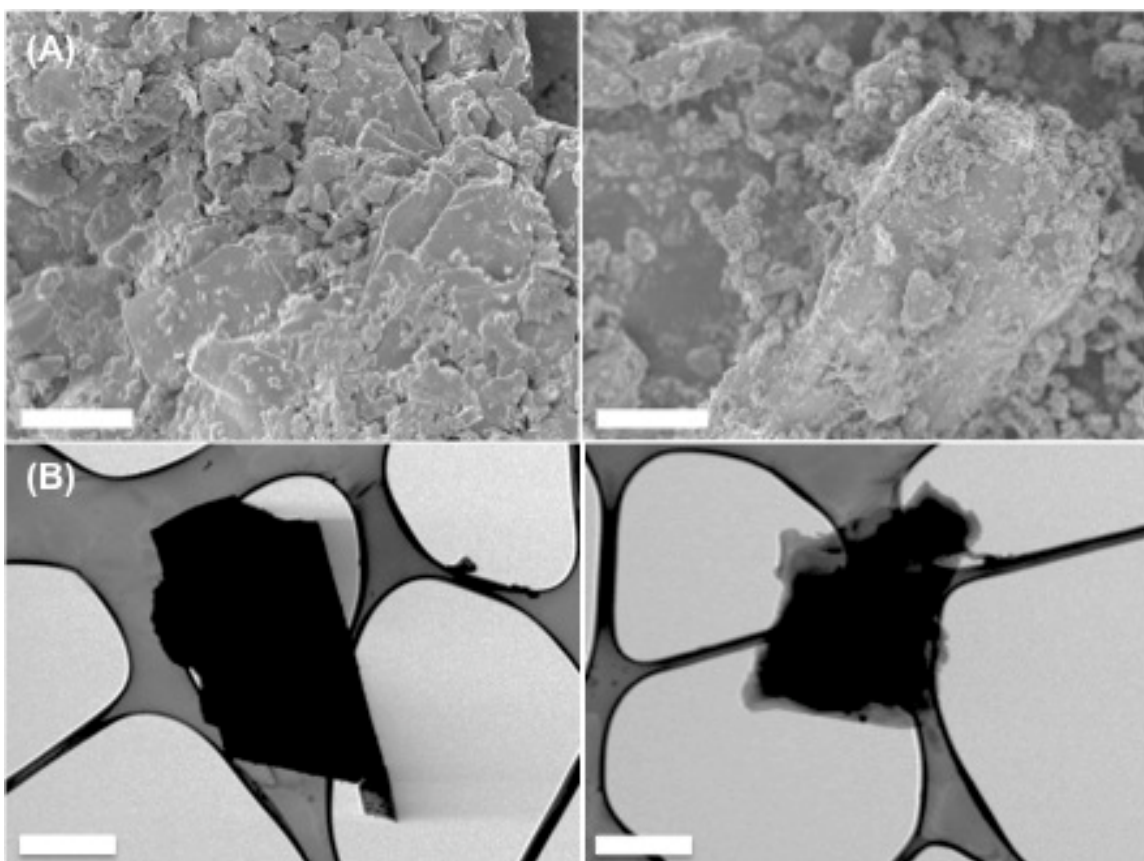


**Figure 1.** Size characterization of GaSe (left) and GeS (right). (A) SEM and (B) STEM images of the nanomaterials at 5000X and 20 000X magnification respectively. The white scale bars represents 5  $\mu\text{m}$  for SEM and 500 nm for STEM images.

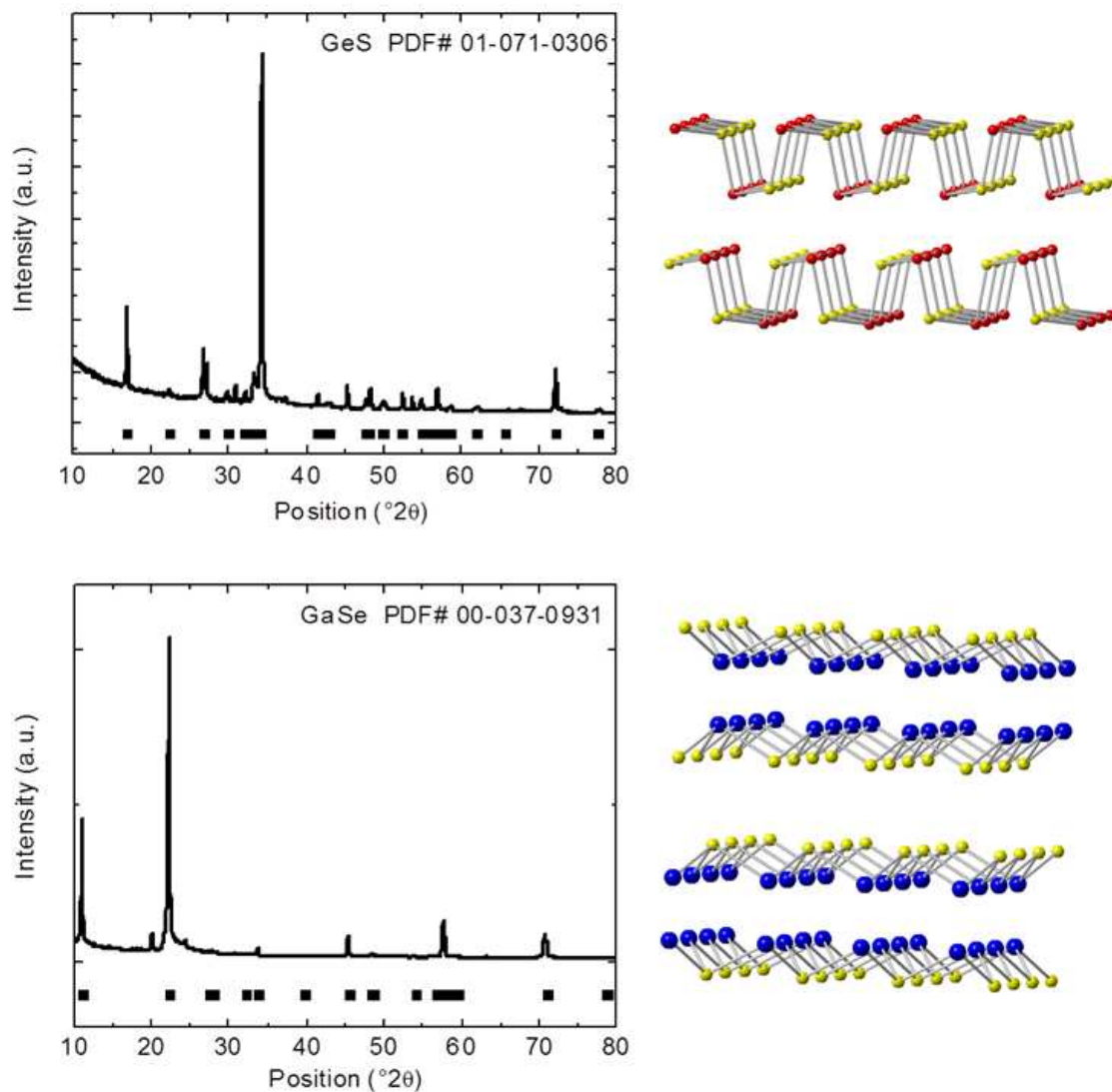


**Figure 2.** X-ray diffractogram of GeS (top) and GaSe (bottom) and corresponding structures (S, Se-yellow, Ge – red, Ga – blue).

### Cytotoxicity assessment of GaSe and GeS

Following 24 h incubation of various concentrations of the GaSe and GeS (between 3.125 to 400  $\mu\text{g/mL}$ ) with A549 cells, WST-8 and MTT cell viability assays were performed to investigate the cytotoxicity of these nanomaterials. Prior to these assessments, the nanomaterials were removed through two washing steps with phosphate buffer solution

(PBS), pH 7.2, so as to reduce any possible interferences of the nanomaterials with the cell viability assays. The active reagent in WST-8 and MTT assays produce orange and purple formazan products respectively after receiving two electrons from dehydrogenases present in metabolically active cells.<sup>22</sup> In the case of WST-8 assay, the formazan product formed is water-soluble, whereas for MTT assay, insoluble formazan crystals were generated. The insoluble formazan crystals can then be dissolved using organic solvents such as dimethyl sulfoxide (DMSO) for spectroscopic analysis. In both WST-8 and MTT assays, the amount of formazan produced is directly proportional to the number of metabolically active cells present.<sup>24</sup> By normalizing the colour intensity of the formazan products formed from cells exposed to varying concentrations of GaSe and GeS with that from a negative control where cells were incubated without any nanomaterials, the extent of cytotoxicity of the nanomaterials can be determined. Due to the different sensitivities of the cell viability reagents in the two assays, cells tested with the WST-8 reagent were incubated for 1 h at 37°C and 5% CO<sub>2</sub>, whereas cells with the MTT reagent were incubated for 3 h at the same conditions.

### **WST-8 assay**

The cytotoxicity of GaSe and GeS was first investigated using the WST-8 assay. Figure 3 shows that both nanomaterials induced concentration-dependent effect on the cell viability of A549 cells. However, they resulted in opposite trends of cell viabilities with increasing dosage of the nanomaterial. While GaSe caused an overall decreasing cell viability with increasing concentration, suggesting that the nanomaterial is toxic, the percentage cell viability derived from the WST-8 assay indicated an increasing cell viability with increasing dosage of GeS nanomaterial. The latter was unexpected of toxic

nanomaterials and thus control experiments were conducted to determine if this peculiar observation was due to the presence of nanomaterial-induced interference on the absorbance measurements.

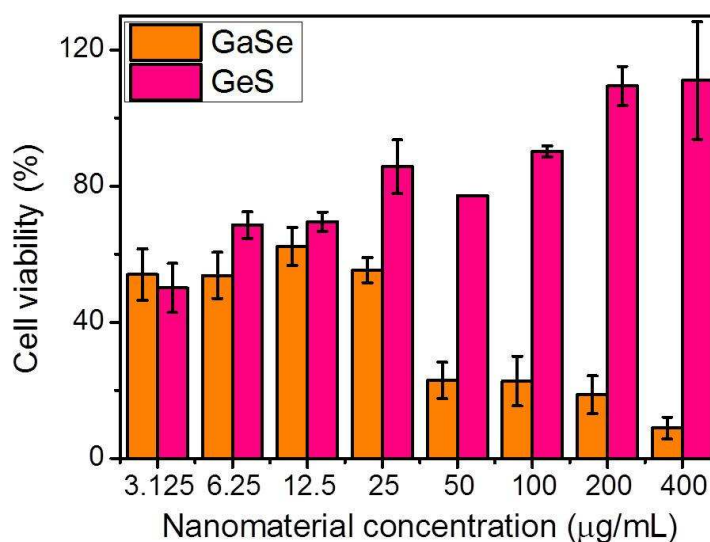


**Figure 3.** Percentage cell viability of A549 cells as measured by WST-8 assay, following 24 h exposure to varying amounts of nanomaterials (GaSe and GeS). The percentages are normalized to data obtained from the negative control that are not exposed to any nanomaterials. These results are mean values with  $\pm$  standard deviations of a minimum of three repeat experiments, each consisting of four wells per treatment for every concentration.

In order to examine for nanomaterials-induced artifacts on WST-8 assay measurements, GaSe and GeS nanomaterials were incubated separately with WST-8 reagent in the absence of cells. In cell-free conditions, an increase in the relative percentage of formazan generated will indicate that the nanomaterials could reduce the WST-8 reagent and interfere with the absorbance measurements, contributing to an overestimation of cell

viability. The relative percentages of formazan formation from GaSe and GeS in cell-free condition are shown in Figure 4.

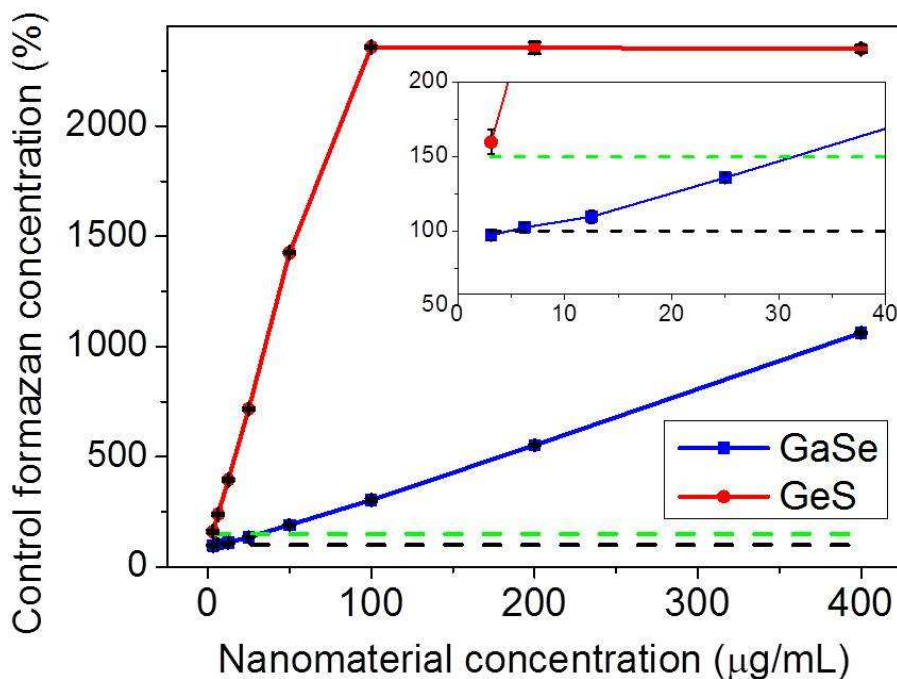


**Figure 4.** Percentage of formazan generated from GaSe and GeS under cell-free conditions, normalized to the amount of formazan generated in the absence of nanomaterials. The graph illustrates the degree of reduction of WST-8 reagent to formazan product with different GaSe and GeS concentrations. The black dotted line represents the blank control where there is no nanomaterial incubated with the WST-8 assay. The green dotted line in the inset represents 150% control formazan concentration limit set, below which interference is considered as insignificant.

From Figure 4, it was observed that both nanomaterials reacted with the WST-8 reagent significantly, with GaSe and GeS resulting in the production of 1062% and 2350% control formazan concentration respectively at the highest concentration (400  $\mu\text{g/mL}$ ) of nanomaterial tested. A plateau in the absorbance intensity was observed for GeS above 100  $\mu\text{g/mL}$ , possibly because WST-8 reagent was the limiting reagent for the reduction

reaction. Between the two nanomaterials, GeS imparted a greater interference as compared to GaSe. This differing extent of artifact-induced interference could have resulted in the opposite cell viability trends observed between GaSe and GeS. Hypothetically, we might assume any nanomaterial to induce significant artifacts on the absorbance measurements if the calculated formazan concentration is beyond  $\pm 50\%$  of the blank control which is free from cells and the nanomaterial of interest. As such, we could deduce from the WST-8 assay control experiments that GaSe and GeS would distort the cell viability data if they existed at concentrations above  $\sim 30 \mu\text{g/mL}$  and  $\sim 3 \mu\text{g/mL}$  (inset in figure 4) in the cell cultures respectively when the WST-8 assay was added. Through careful repeated washings prior to the addition of WST-8 assay for our cell viability assessments, the amount of nanomaterial left in the cell culture that could react with the WST-8 assay should be reduced drastically, to around  $25 - 50 \mu\text{g/mL}$  for the highest concentration of nanomaterial introduced ( $400 \mu\text{g/mL}$ ). For GaSe, these residual amounts are unlikely to cause interferences for concentrations tested between  $3.125$  to  $200 \mu\text{g/mL}$ . However, for GeS, similar residual amounts after performing the same washing procedure can still impart significant interference effects for all concentrations tested due to its higher reducing activity with the WST-8 assay reagent as compared to GaSe. Therefore, it is highly probable that the cell viability measurements of GeS was affected by interference from the nanomaterial, leading to the perceived trend of higher cell viability with increased dosage of GeS incubated.

### **MTT assay**

In order to verify the validity of the cell viability data obtained from the WST-8 assay, a second cell viability assay (MTT) was used to assess the cytotoxicity of GaSe and GeS



(Figure 5). Similar to the results obtained for WST-8 assay, GaSe displayed dose-dependent toxicological effect on A549 cells while GeS continued to give high cell viability values at the highest concentration (400  $\mu\text{g/mL}$ ) exposed.

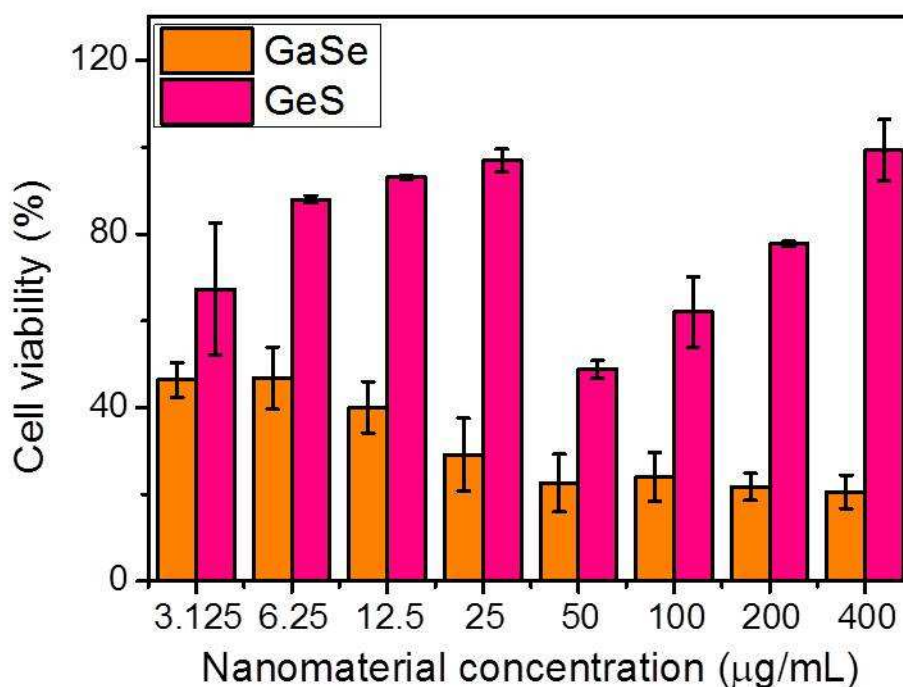


**Figure 5.** Percentage cell viability of A549 cells as measured by MTT assay, following 24 h exposure to varying amounts of GaSe and GeS. The percentages are normalized to data obtained from the negative control that are not exposed to any nanomaterials. These results are mean values with  $\pm$  standard deviations of a minimum of three repeat experiments, each consisting of four wells per treatment for every concentration.

Two control experiments were carried out to identify possible nanomaterial-induced interferences on the MTT cell viability measurements. The first control experiment was to test for possible binding of the nanomaterials to the insoluble formazan crystals and subsequent removal of these crystals after centrifugation. Ascorbic acid, a substance

known to reduce tetrazolium compounds to formazan<sup>25</sup>, was added to the MTT-nanomaterial mixtures after 3 h incubation to preferentially generate the insoluble formazan crystals for this investigation. In the event that the relative percentage control formazan concentration of the MTT-nanomaterial-ascorbic acid mixture is significantly lower than 100%, it could be inferred that there is sufficient binding between the formazan crystals and the nanomaterials. The second control experiment was similar to that conducted for WST-8, which examined the possibility of the reduction of MTT reagent by the nanomaterial to form formazan products in the absence of cells. The results from these MTT control experiments are illustrated in Figure 6.

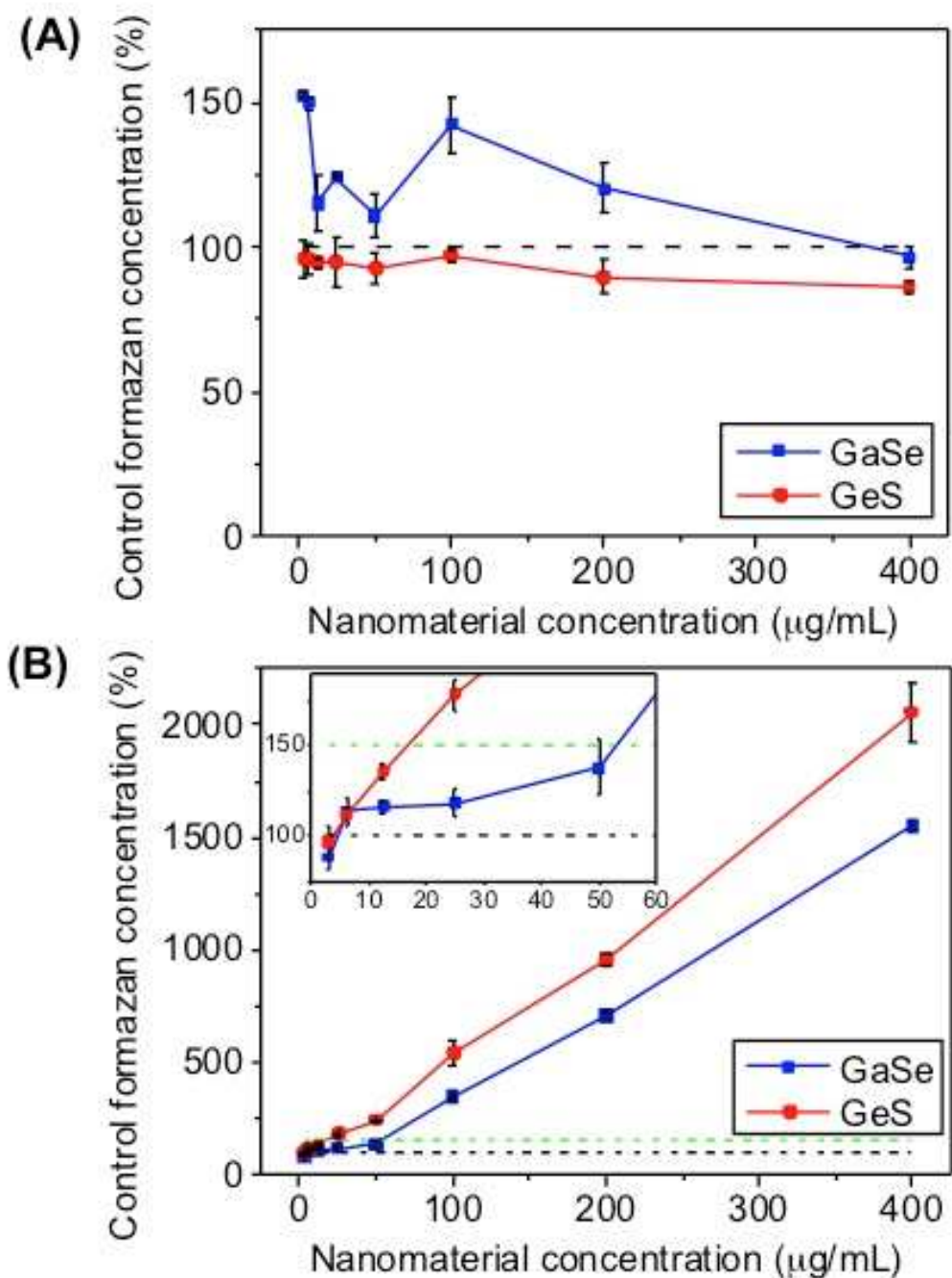


**Figure 6.** Percentage of formazan generated from GaSe and GeS under cell-free conditions, normalized to the amount of formazan generated in the absence of nanomaterials. Graph A shows the level of binding between MTT formazan products with the nanomaterials. Graph B shows the degree of reduction of MTT reagent to formazan product with varying GaSe and GeS concentrations. The black dotted line represents

the blank control where there is no nanomaterial incubated with the MTT assay. The green dotted line in the inset in Graph B represents 150% control formazan concentration limit set, below which interference is considered as insignificant.

Binding effects between the nanomaterials and the MTT formazan crystals has been reported to prevent the dissolution of the formazan formed by the organic solvent used, thereby giving an inflated cytotoxicity response.<sup>25</sup> Since the relative percentage control formazan concentration values in Figure 6A did not show any significant reduction below 100% for both nanomaterials, it was deduced that there was negligible interference due to this binding effect. However, both nanomaterials were found to cause significant reduction of the MTT reagent (Figure 6B), similar to that for WST-8 reagent. GaSe and GeS resulted in the production of 1548% and 2054% control formazan concentration respectively, at the highest dosage of 400  $\mu\text{g/mL}$  tested. Figure 6B also showed that between the two nanomaterials, GeS would cause greater interference to the MTT cell viability measurements as compared to GaSe. In the same manner, we could infer from the data attained in Figure 6B that GeS and GaSe would distort the MTT cell viability results at concentrations above  $\sim 15 \mu\text{g/mL}$  and  $\sim 50 \mu\text{g/mL}$  respectively, if we regard 150% percentage formazan concentration to be the threshold for significant interference (inset in figure 6B). For GaSe, the thorough washing steps performed on the cell culture to remove the nanomaterials before the addition of the MTT assay should render little nanomaterial-induced artifact for all concentrations tested. In the case of GeS, despite the same washing steps performed, its cytotoxicity data as derived from the MTT assay measurements could still be affected by the generation of excess MTT formazan crystals from the reaction between GeS and the MTT reagent, especially for the higher amounts

of GeS, as evident from the percentage cell viability values in Figure 5. Thus, the cytotoxicity of GeS in both WST-8 and MTT assays is underestimated and erroneous.

Based on the percentage cell viability values in both WST-8 and MTT assays measurements, it was observed that GaSe is relatively toxic, with 46% (WST-8) and 54% (MTT) viable cells remaining after 24 h exposure to the lowest dosage (3.125  $\mu\text{g/mL}$ ) of nanomaterial treated, where the interference effect on the absorbance measurements by residual amounts of nanomaterial following careful washings is minimal. In addition, it was found that GaSe exhibited much higher toxicity when compared to many other well-known chalcogenides such as  $\text{MoS}_2$ ,  $\text{WS}_2$  and  $\text{WSe}_2$  (Figure 7).<sup>24</sup> This difference in toxicities may be attributed to the higher *in vitro* solubility of gallium ions compared to transition metals at physiological pH. This is supported by previous studies where compounds with higher *in vitro* solubility showed greater toxicity.<sup>26</sup> Besides higher *in vitro* solubility, involvement of a variety of other factors such as different synthesis methods, particle characteristics and physicochemical properties can also affect the toxicity of the nanomaterial.<sup>27-31</sup>

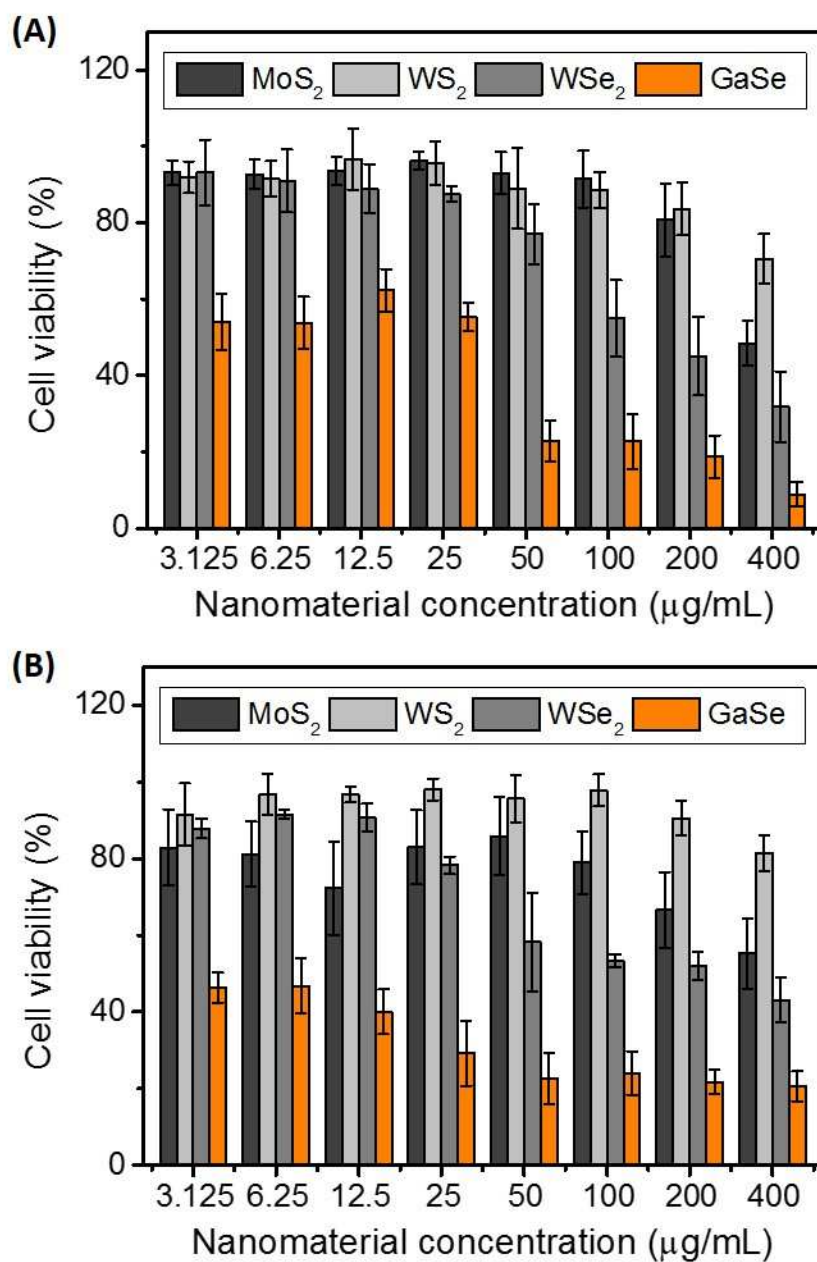


Figure 7: Comparison of cell viability measurements using (A) WST-8 and (B) MTT assays between GaSe and various transition metal chalcogenides (TMDs; MoS<sub>2</sub>, WS<sub>2</sub>, WSe<sub>2</sub>) across different nanomaterial concentrations, after 24 h exposure with A549 cells. Data presented for TMDs are obtained Reference 24. Note that these TMDs can also

reduce the MTT reactive agent, however, in a much lesser extent compared to GaSe. The same washing procedures were conducted for the TMDs, ensuring comparable and almost interference-free cell viability data.

## Conclusion

In view of the rising research on the applications of GaSe and GeS, we conducted an *in vitro* cytotoxicity assessment of these semiconductor chalcogenides to determine if these materials may have an adverse effect on our wellbeing if they were to be commercialized in the future. GaSe and GeS were incubated with A549 cells for 24 h and cell viability measurements were performed thereafter using WST-8 and MTT assays. The cytotoxicity results obtained showed that GaSe is significantly more toxic than transition metal dichalcogenides (MoS<sub>2</sub>, WS<sub>2</sub>, WSe<sub>2</sub>). GeS, on the other hand, appeared to be non-toxic, with concentration having a positive correlation with cell viability. Control experiments under cell-free conditions revealed significant interferences between both nanomaterials and the assay reagents, with GeS showing greater interferences than GaSe. In view of this, other cell viability assays should be explored to study the cytotoxicity effects of GaSe and GeS more accurately. As toxicity studies of GaSe and GeS are still in its infancy, more research can be done to determine their effects on our health so as to ensure our safety before their actual commercial application.

## Acknowledgements

M. P., A. C. F and N. L. thank C4T programme for funding. This project was funded by the National Research Foundation Singapore under its Campus for Research Excellence

and Technological Enterprise (CREATE) programme. Z.S. and Š.H. were supported by Czech Science Foundation (GACR No. 15-07912S).

## References:

- 1 W. Jie, X. Chen, D. Li, L. Xie, Y. Y. Hui, S. P. Lau, X. Cui and J. Hao, *Angew. Chem. Int. Ed. Engl.*, 2015, **54**, 1185–1189.
- 2 S. Lei, L. Ge, Z. Liu, S. Najmaei, G. Shi, G. You, J. Lou, R. Vajtai and P. M. Ajayan, *Nano Lett.*, 2013, **13**, 2777–2781.
- 3 Y. Ma, Y. Dai, M. Guo, L. Yu and B. Huang, *Phys. Chem. Chem. Phys.*, 2013, **15**, 7098–7105.
- 4 D. V. Rybkovskiy, N. R. Arutyunyan, A. S. Orekhov, I. A. Gromchenko, I. V. Vorobiev, A. V. Osadchy, E. Y. Salaev, T. K. Baykara, K. R. Allakhverdiev and E. D. Obraztsova, *Phys. Rev. B*, 2011, **84**, 085314.
- 5 P. Hu, Z. Wen, L. Wang, P. Tan and K. Xiao, *ACS Nano*, 2012, **6**, 5988–5994.
- 6 O. I. Aksimentyeva, P. Y. Demchenko, V. P. Savchyn and O. A. Balitskii, *Nanoscale Res. Lett.*, 2013, **8**, 29–33.
- 7 S. Murugesan, P. Kearns and K. J. Stevenson, *Langmuir*, 2012, **28**, 5513–5517.
- 8 L. Makinistian and E. A. Albanesi, *Phys. Rev. B*, 2006, **74**, 045206.
- 9 Y. J. Cho, H. S. Im, Y. Myung, C. H. Kim, H. S. Kim, S. H. Back, Y. R. Lim, C. S. Jung, D. M. Jang, J. Park, E. H. Cha, S. H. Choo, M. S. Song and W. II Cho, *Chem. Commun.*, 2013, **49**, 4661–4663.
- 10 C. Li, L. Huang, G. P. Snigdha, Y. Yu and L. Cao, *ACS Nano*, 2012, **6**, 8868–8877.
- 11 D. D. Vaughn II, R. J. Patel, M. A. Hickner and R. E. Schaak, *J. Am. Chem. Soc.*, 2010, **132**, 15170–15172.
- 12 L. Shi and Y. J. Dai, *J. Appl. Cryst.*, 2014, **47**, 527–531.
- 13 H. Peng, S. Meister, C. K. Chan, X. F. Zhang and Y. Cui, *Nano Lett.*, 2007, **7**, 199–203.
- 14 D. J. Late, B. Liu, J. Luo, A. Yan, H. S. S. R. Matte, M. Grayson, C. N. R. Rao and V. P. Dravid, *Adv. Mater.*, 2012, **24**, 3549–3554.



- 
- 15 P. M. Ndangili, A. N. Jijana, R. A. Olowu, S. N. Mailu, F. R. Ngece, A. Williams, T. T. Waryo, P. G. L. Baker and E. I. Iwuoha, *Int. J. Electrochem. Sci.*, 2011, **6**, 1438-1453.
- 16 S. Cui, R. Chahal, C. Boussard-Plédel, V. Nazabal, J. Doualan, J. Troles, J. Lucas and B. Bureau, *Molecules*, 2013, **18**, 5373-5388.
- 17 M. Pumera, *Chem Asian J.* 2011, **6**, 340.
- 18 A. Tanaka, M. Hirata, M. Shiratani, K. Koga and Y. Kiyohara, *J. Occup. Health*, 2012, **54**, 187-195.
- 19 D. L. Morgan, C. J. Shines, S. P. Jeter, M. E. Blazka, M. R. Elwell, R. E. Wilson, S. M. Ward, H. C. Price and P. D. Moskowitz, *Toxicol. Appl. Pharmacol.*, 1997, **147**, 399-410.
- 20 G. B. Gerber and A. Léonard, *Mutat. Res.*, 1997, **387**, 141-146.
- 21 S. H. Tao and P. M. Bolger, *Regul. Toxicol. Pharmacol.*, 1997, **25**, 211-219.
- 22 D. Richards and A. Ivanisevic, *Chem. Soc. Rev.*, 2012, **41**, 2052-2060.
- 23 B. Kong, J. H. Seog, L. M. Graham and S. B. Lee, *Nanomedicine (Lond.)*, 2011, **6**, 929-941.
- 24 W. Z. Teo, E. L. Chng, Z. Sofer and M. Pumera, *Chem.-Eur. J.*, 2014, **20**, 9627-9632.
- 25 L. Belyanskaya, P. Manser, P. Spohn, A. Bruinink and P. Wick, *Carbon*, 2007, **45**, 2643-2648.
- 26 D. L. Morgan, C. J. Shines, S. P. Jeter, R. E. Wilson, M. P. Elwell, H. C. Price and P. D. Moskowitz, *Environ. Res.*, 1995, **71**, 16-24.
- 27 Y.-W. Huang, C.-H. Wu and R. S. Aronstam, *Materials*, 2010, **3**, 4842-4859.
- 28 E. L. K. Chng and M. Pumera, *RSC Adv.*, 2015, **5**, 3074-3080.
- 29 E. L. K. Chng, Z. Sofer and M. Pumera, *Nanoscale*, 2014, **6**, 14412-14418.
- 30 W. Z. Teo, E. L. K. Chng, Z. Sofer and M. Pumera, *Nanoscale*, 2014, **6**, 1173-1180.
- 31 E. L. K. Chng and M. Pumera, *Chem.-Eur. J.*, 2013, **19**, 8227-8235.



201x125mm (96 x 96 DPI)